



Dissolution-precipitation reactions controlling fast formation of dolomite under hydrothermal conditions



German Montes-Hernandez ^{a, b, *}, Nathaniel Findling ^{a, b}, François Renard ^{a, b, c}

^a CNRS, ISTerre, F-38041 Grenoble, France

^b Univ. Grenoble Alpes, ISTerre, F-38041 Grenoble, France

^c PGP, Department of Geosciences, University of Oslo, Box 1048 Blindern, 0316 Oslo, Norway

ARTICLE INFO

Article history:

Received 14 May 2016

Received in revised form

21 August 2016

Accepted 23 August 2016

Available online 26 August 2016

Keywords:

Dolomite

Mg-calcite

Ca-magnesite

Hydrothermal conditions

CO₂

Carbonation

ABSTRACT

In laboratory experiments, the precipitation of dolomite at ambient temperature is virtually impossible due to strong solvation shells of magnesium ions in aqueous media and probably also due to the existence of a more intrinsic crystallization barrier that prevents the formation of long-range ordered crystallographic structures at ambient surface conditions. Conversely, dolomite can easily form at high temperature (>100 °C), but its precipitation and growth requires several days or weeks depending on experimental conditions. In the present study, experiments were performed to assess how a single heat-ageing step promotes the formation of dolomite under high-carbonate alkaline conditions via dissolution-precipitation reactions. This reaction pathway is relevant for the so-called hydrothermal dolomite frequently observed in carbonate platforms, but still ill-defined and understood. Our precipitation route is summarized by two main sequential reactions: (1) precipitation of Mg-calcite at low temperature (~20 °C) by aqueous carbonation of synthetic portlandite (Ca(OH)₂) in a highly alkaline medium (1 M of NaOH and 1 M of MgCl₂), leading to precipitation of oriented nanoparticles of low- and high-Mg calcite (~79 wt%) coexisting with aragonite (~18 wt%) and brucite (~3 wt%) after 24 h; (2) fast dolomitization process starting from 1 h of reaction by a single heat-ageing step from ~20 to 200, 250 and 300 °C. Here, the Mg-calcite acts as a precursor that lowers the overall kinetics barrier for dolomite formation. Moreover, it is an important component in some bio-minerals (e.g. corals and seashells). Quantitative Rietveld refinements of XRD patterns, FESEM observations and FTIR measurements on the sequentially collected samples suggest fast dolomite precipitation coupled with dissolution of transient mineral phases such as low-Mg calcite (Mg < 4 mol%), high-Mg calcite (Mg > 4 mol%), proto-dolomite (or disordered dolomite; Mg > 40 mol%) and Ca-magnesite. In this case, the dolomite formation rate and the time-dependent mineral composition strongly depend on reaction temperature. For example, high-purity dolomitic material (87 wt% of dolomite mixed with 13 wt% of magnesite) was obtained at 300 °C after 48 h of reaction. Conversely, a lower proportion of dolomite (37 wt%), mixed with proto-dolomite (43 wt%), Ca-magnesite (16 wt%) and high-Mg calcite (4 wt%), was obtained at 200 °C after 72 h. The present experiments provide an additional mechanism for the massive dolomite formation in sedimentary environments (ex. deep sea organic-rich carbonate-sediments) if such sediments are subjected to significant temperature variations, for example by hot fluid circulations related to volcanic activity. In such systems, organic degradation increases the carbonate alkalinity (HCO₃⁻) necessary to induce the dolomitization process at low and high temperature.

© 2016 Elsevier Ltd. All rights reserved.

1. Introduction

The formation and structural properties of dolomite (CaMg(CO₃)₂) have been investigated in the past two centuries because this mineral can be found throughout the Earth's crust and

is associated with several elements of economic importance (including the so-called rare earth elements) and hydrocarbon deposits (e.g. McKenzie, 1991; Warren, 2000; Davies and Smith, 2006; Sanchez-Roman et al., 2009; McKenzie and Vasconcelos, 2009; Deelman, 2011; Xu et al., 2013). However, various questions still remain debated concerning the formation mechanisms and kinetics of dolomite in natural systems as well as its synthesis in the laboratory. Moreover, the scanty distribution of recent dolomite in

* Corresponding author. CNRS, ISTerre, F-38041 Grenoble, France.

E-mail address: german.montes-hernandez@ujf-grenoble.fr (G. Montes-Hernandez).

natural environments contrasts strongly with its abundance in ancient sedimentary rocks of marine origin, leading to the paradox commonly referred to as the “dolomite problem” (Compton, 1988; Arvidson and Mackenzie, 1997, 1999). Dolomite is a complex mineral because it can precipitate either via a diagenetic mineral replacement mechanism or through hydrothermal and/or metamorphic mechanisms. For all these mechanisms, fluid flow and sufficient magnesium in the interacting fluid are required. This complexity has been debated in recent decades and has led to various interpretations on the origin of dolomite in geological formations (Warren, 2000; Mckenzie and Vasconcelos, 2009; Jacquemyn et al., 2014).

It has been observed that dolomite can form in lakes, on or beneath shallow seafloors, in zones of brine reflux and in early to late burial settings (Warren, 2000). More recently, various studies have proposed that bacterial metabolism may aid the process of dolomite nucleation and precipitation in shallow environments such as hypersaline anoxic lakes where the presence of sulfate-reducing conditions and microbial activity are observed (e.g. Warren, 2000; Warthmann et al., 2000; Kenward et al., 2009; Deng et al., 2010). In addition, hot hydrothermal fluids may circulate in carbonate platforms during burial diagenesis. Fluid temperature may increase via volcanic activity (e.g. igneous intrusions, sill and dike emplacement), and hydrothermal systems could be created at a local and/or regional scale (e.g. Blendinger, 2004; Davies and Smith, 2006; Jacquemyn et al., 2014). In such cases, the replacement of limestone by dolomite could be significantly enhanced if sufficient amounts of magnesium are supplied to the system (Jacquemyn et al., 2014). Under such burial conditions, magnesium could originate from various sources, such as seawater, dissolution of ultrabasic rocks (when igneous intrusions and/or hydrothermalism are present), and dissolution of preexistent Mg-carbonates (e.g. low and high Mg-calcite, magnesite, brucite and proto-dolomite) contained in fossil organisms (e.g. seashells, corals and coralline algae) abundant in carbonate platforms. In these non-equilibrated systems, organic degradation can also lead to a significant increase in the carbonate alkalinity ($2\text{CH}_2\text{O}$ (organic matter) + $\text{SO}_4^{2-} \rightarrow \text{H}_2\text{S} + 2\text{HCO}_3^-$) of interacting fluids via bacterial and/or thermochemical sulfate reduction (e.g. Compton, 1988; Warren, 2000; Machel, 2001; Nash et al., 2011).

High carbonate alkalinity and temperature are crucial parameters to enhance the dolomitization processes in natural hydrothermal systems (Machel, 2001; Jacquemyn et al., 2014), as recently demonstrated in the laboratory (Montes-Hernandez et al., 2014). In this context, the so-called hydrothermal dolomite (HTD), as defined by Davies and Smith (2006), was observed in several carbonate formations, for example, in the Devonian and Mississippian of the Western Canada sedimentary basin, in the Ordovician of the Michigan and Appalachian basins of eastern Canada and north-eastern United States, in the Cretaceous of onshore and offshore Spain, in the Anisian-Ladinian Latemar platform of northern Italy and many other locations (Davies and Smith, 2006; Jacquemyn et al., 2014 and references therein). In these studies, stable isotopes of oxygen (^{18}O) and carbon (^{13}C), fluid inclusion rehomogenization temperature and salinity and petrographic/textural criteria were used to discriminate low-temperature dolomite from hydrothermal dolomite ($>80^\circ\text{C}$). The presence of superstructure-ordering reflections in X-ray diffraction spectra, as previously defined by Lippmann (1973), is the main characteristic of hydrothermal dolomite. However, this simple crystallographic criterion is rarely used. Accordingly, at low temperature only disordered dolomite (or proto-dolomite) can be formed, as discussed below. In the present study, several laboratory experiments were performed to assess how a single heat-ageing step promotes the formation of ordered dolomite (i.e. with superstructure-

ordering reflection in XRD patterns) under high-carbonate alkaline conditions via dissolution-precipitation reactions.

Experimental physicochemical conditions, reaction mechanisms and kinetics at which dolomite can be formed provide new insights for a better understanding of dolomite formation. Several studies have demonstrated that the formation of dolomite at ambient temperature is virtually impossible or that geological time scales are probably required (Deelman, 2001; Pimentel and Pina, 2014). This limitation has been related to the strong solvation shells of magnesium ions in aqueous media; a similar situation exists for magnesite (MgCO_3) which raises the same difficulty of precipitating at room temperature and atmospheric pressure in laboratory experiments (Deelman, 2001, 2011; Xu et al., 2013). A recent study reported on the synthesis of MgCO_3 and $\text{Mg}_x\text{Ca}_{1-x}\text{CO}_3$ ($0 < x < 1$) solid phases at ambient conditions in the absence of water, i.e. using formamide as solvent (Xu et al., 2013). This study suggests the existence of a more intrinsic crystallization barrier that prevents the formation of long-range ordered crystallographic structures ($R\bar{3}2/c$ in magnesite and $R\bar{3}$ in dolomite) at ambient conditions.

On one hand, various authors have claimed that dolomite formation at ambient laboratory conditions is possible by using bio-assisted systems. In such studies, sulfate-reducing or aerobic heterotrophic bacteria, hypersaline or seawater solutions and anoxic or oxic conditions have been used (e.g. Warthmann et al., 2000; Sanchez-Roman et al., 2009; Kenward et al., 2009; Deng et al., 2010; Krause et al., 2012). However, the reported X-ray diffraction patterns do not clearly show the presence of the superstructures characteristic of dolomite (ordering reflections at 22.02 (101), 35.32 (015), 43.80 (021), etc. 2θ , see Lippmann (1973)). These superstructure reflections are related to the alternating regular monolayers of Ca and Mg perpendicular to the c -axis of ordered dolomite crystals.

On the other hand, ordered dolomite can be synthesized at higher temperatures ($>100^\circ\text{C}$) by mixing (fast or slowly) two pre-defined solutions, one containing Mg/Ca (ratio ≥ 1) and the other containing dissolved carbonate ions (Medlin, 1959; Arvidson and Mackenzie, 1999; Deelman, 2001), or by placing high-purity calcite or limestone material in contact with Mg-rich solutions (Grover and Kubanek, 1983; Dockal, 1988; Kaczmarek and Sibley, 2011; Etschmann et al., 2014; Jonas et al., 2015). Both synthesis methods require several days or weeks depending on experimental conditions. Therefore, identifying novel and/or innovative abiotic or biotic synthesis methods for dolomitic materials under a broad spectrum of experimental conditions remains a major challenge in order to obtain a better understanding of its formation in natural systems.

In a previous study, it was demonstrated that ordered dolomite can be precipitated via simultaneous dissolution of calcite and magnesite under hydrothermal conditions between 100 and 200°C (Montes-Hernandez et al., 2014). The high-carbonate alkalinity in the interacting solution significantly promoted the formation of dolomite with respect to pure water as initial interacting fluid. However, about 90 days were required to obtain 50% of ordered dolomite in the solid at 200°C . Based on this previous study, new experimental conditions are explored here using semi-continuous dispersed reactors. In these experiments, high-magnesium calcite is first produced at ambient temperature, maintaining a constant carbonate alkalinity. The Mg-calcite produced acts as a precursor for the dolomitization process when a fast heating step occurs in the system, mimicking for example, volcanic activity or the circulation of hot ($200\text{--}300^\circ\text{C}$) fluids in the crust. Under these conditions, the precipitation of dolomite can be very fast. In addition, various aliquots of suspensions were withdrawn from the reactor as a function of time in order to obtain specific information on the kinetics and reaction mechanism. With

this new protocol, dolomite minerals can be produced much faster, within two days. The dolomite formation rate and time-dependent mineral composition were then deduced from quantitative Rietveld refinement of x-ray diffraction (XRD) patterns. These kinetic data are also supported by FESEM observations and FTIR measurements on solids and by ICP-AES element chemical analyses in the interacting solutions for calcium and magnesium. Finally, brucite mineral ($\text{Mg}(\text{OH})_2$) was also tested as a magnesium source in complementary experiments.

2. Materials and methods

2.1. Precipitation of dolomite ($\text{MgCa}(\text{CO}_3)_2$)

250 ml of high-purity water with electrical resistivity of 18.2 M Ω cm, 0.25 mol of NaOH, 0.25 mol of $\text{MgCl}_2 \cdot 6\text{H}_2\text{O}$ and 0.25 mol of synthetic portlandite ($\text{Ca}(\text{OH})_2$) were placed in a reactor (Hastelloy C22 autoclave with internal volume of 0.6 L). This reactive suspension was continually stirred during the reaction by means of a constant mechanical stirring system (400 rpm). The temperature of the suspension increased instantaneously to 26 °C due to the exothermic dissolution of NaOH in the system. At this reference temperature, CO_2 (≈ 0.62 mol) was immediately injected in the system at a pressure of 44 bar. The carbonation reaction started instantaneously as attested by the continuous consumption of CO_2 , reflected by a pressure drop in the system, and an increase in temperature during the exothermic carbonation reaction (the maximum temperature reached ≈ 29 °C after 1 h of reaction ($\Delta T \approx 3$ °C)). After 24 h of carbonation reaction at ambient temperature (19–21 °C) (including the exothermic period), a heat-ageing step was performed from ambient temperature to 200, 250 and 300 °C. About 10 mL of the dispersion was then sampled in the reactor as a function of time during the nucleation and growth of dolomite. For these three different temperature conditions, the dispersion was typically collected

after 1, 3, 5, 8, 24, and 48 h in each experiment. The experiment performed at 200 °C was prolonged up to 72 h. The collected/withdrawn dispersion was first cooled by water circulation in the sampling system. Then, all collected-time samples were carefully recovered and separated by centrifugation (30 min at 12,000 rpm), decanting the supernatant solutions. The solid product was washed twice by re-dispersion/centrifugation processes in order to remove the soluble salts formed during the synthesis and susceptible to precipitate during drying (sodium carbonates and NaCl). Finally, the solid product was dried directly in the centrifugation flasks at 90 °C for 24 h. The dry solid product was manually recovered and stored in plastic flasks for subsequent characterization (FESEM, XRD and FTIR).

Additional batch experiments, i.e. without suspension sampling as a function of time, were carried out in order to obtain information on the role of NaOH (presence or absence), Mg source (MgCl_2 or $\text{Mg}(\text{OH})_2$) and temperature (sequential heat-ageing steps in the same experiment: from 20 to 90 °C, from 90 to 200° and from 200 to 300 °C, with each step having a minimum duration of 24 h). The experimental conditions and mineral composition of the solid products of all of the syntheses are indicated in Table 1.

2.2. Characterization of the solid products

X-Ray Powder Diffraction (XRD) analyses were performed using a Siemens D5000 diffractometer in Bragg-Brentano geometry, equipped with a theta-theta goniometer with a rotating sample holder. The XRD patterns were collected using $\text{Cu } \alpha_1$ ($\lambda_{\text{Cu}\alpha_1} = 1.5406$ Å) and α_2 ($\lambda_{\text{Cu}\alpha_2} = 1.5444$ Å) radiation in the range $2\theta = 10$ – 70° with a step size of 0.04° and a counting time of 6 s per step. Magnesium calcite ($0 \leq \text{Mg content} \leq 50$ mol%), calcium magnesite ($0 \leq \text{Ca content} \leq 50$ mol%), brucite, aragonite, and dolomite minerals were systematically refined by the quantitative Rietveld method on XRD patterns using the BGMN software and its associated database (Taut et al., 1998). Concerning calcite and

Table 1
Summary of experimental conditions and mineral composition of solid products.

| Run | t (h) | T (°C) | P (bar) | Mineral composition (wt%) from rietveld refinement of XRD patterns | | | | | | | | |
|-------|----------------|--------|---------|--|----|-----------|----------|-----------|----------|----|---------|------------------|
| | | | | A | B | High-Mg C | Low-Mg C | High-Ca M | Low-Ca M | M | Proto-D | Ordered dolomite |
| Dol6 | 0 ^a | 20 | 17 | 18 | 3 | 45 | 34 | 0 | 0 | 0 | 0 | 0 |
| | 1 | 300 | 100 | 5 | 4 | 0 | 7 | 23 | 0 | 0 | 61 | 0 |
| | 3 | 300 | 100 | 0 | 0 | 2 | 0 | 27 | 0 | 0 | 32 | 39 |
| | 5 | 300 | 100 | 0 | 0 | 2 | 0 | 23 | 0 | 0 | 24 | 51 |
| | 8 | 300 | 100 | 0 | 0 | 0 | 0 | 0 | 21 | 0 | 25 | 54 |
| | 23 | 300 | 100 | 0 | 0 | 0 | 0 | 0 | 19 | 0 | 0 | 81 |
| Dol7 | 48 | 300 | 100 | 0 | 0 | 0 | 0 | 0 | 0 | 13 | 0 | 87 |
| | 1.5 | 200 | 54 | 0 | 10 | 0 | 16 | 26 | 0 | 0 | 20 | 28 |
| | 5 | 200 | 50 | 0 | 0 | 5 | 0 | 47 | 0 | 0 | 28 | 20 |
| | 24 | 200 | 49 | 0 | 0 | 3 | 0 | 48 | 0 | 0 | 19 | 30 |
| | 48 | 200 | 45 | 0 | 0 | 2 | 0 | 49 | 0 | 0 | 18 | 31 |
| Dol8 | 72 | 200 | 43 | 0 | 0 | 4 | 0 | 17 | 0 | 0 | 42 | 37 |
| | 1 | 250 | 58 | 0 | 32 | 11 | 27 | 13 | 0 | 0 | 0 | 17 |
| | 5 | 250 | 57 | 0 | 0 | 6 | 4 | 46 | 0 | 0 | 0 | 44 |
| | 9 | 250 | 57 | 0 | 0 | 0 | 0 | 49 | 0 | 0 | 0 | 51 |
| | 24 | 250 | 56 | 0 | 0 | 0 | 0 | 45 | 0 | 0 | 0 | 55 |
| Dol9* | 48 | 250 | 55 | 0 | 2 | 0 | 4 | 30 | 0 | 0 | 0 | 64 |
| | 96 | 90 | 11 | 10 | 37 | 20 | 21 | 6 | 0 | 0 | 6 | 0 |
| | 24 | 200 | 33 | 8 | 1 | 33 | 2 | 34 | 0 | 0 | 22 | 0 |
| | 30 | 300 | 95 | 0 | 20 | 7 | 4 | 0 | 0 | 0 | 18 | 51 |
| Dol10 | 48 | 300 | 133 | 0 | 0 | 0 | 0 | 0 | 0 | 35 | 0 | 65 |
| | 72 | 300 | 117 | 0 | 0 | 0 | 4 | 0 | 0 | 5 | 16 | 75 |
| Dol11 | 72 | 300 | 128 | 0 | 0 | 31 | 20 | 0 | 0 | 49 | 0 | 0 |

Dol6-to-Dol9: $\text{Ca}(\text{OH})_2$ - MgCl_2 -NaOH- H_2O - CO_2 system; *: three sequential heat-ageing steps; Dol10: $\text{Ca}(\text{OH})_2$ - MgCl_2 - H_2O - CO_2 system (in absence of NaOH); Dol11: $\text{Ca}(\text{OH})_2$ - $\text{Mg}(\text{OH})_2$ -NaOH- H_2O - CO_2 system (MgCl_2 changed by $\text{Mg}(\text{OH})_2$); Dol12: $\text{Ca}(\text{OH})_2$ - $\text{Mg}(\text{OH})_2$ - H_2O - CO_2 system (in absence of NaOH and MgCl_2 changed by $\text{Mg}(\text{OH})_2$), t: reaction duration; a: mineral composition prior to heat-ageing step; T: reaction temperature; P: total pressure (at high temperature CO_2 + H_2O vapor); A: Aragonite; B: brucite; High-Mg C: magnesium calcite ($\text{Mg} > 4$ mol%); Low-Mg C: magnesium calcite ($\text{Mg} < 4$ mol%); High-Ca M: calcium magnesite ($\text{Ca} > 4$ mol%); Low-Ca M: calcium magnesite: ($\text{Ca} < 4$ mol%); M: magnesite; Proto-D: proto-dolomite ($\text{Mg} > 40$ mol%) or disorder dolomite.

magnesite minerals, five crystalline solid solutions were defined from the Rietveld refinements results depending on the magnesium content in calcite 1) low-Mg calcite (<4 mol%), 2) high-Mg calcite (>4 mol%) and 3) proto-dolomite (Mg > 38 mol%) or disordered dolomite) or on the calcium content in magnesite (4) low-Ca magnesite (<4 mol%) and 5) high-Ca magnesite (>4 mol%). We note that the so-called proto-dolomite in our study corresponds to a very-high Mg calcite where magnesium content is: $38 \leq \text{Mg content} \leq 50$ mol% and the superstructure-ordering reflections in the experimental diffractogram are absent.

2.2.1. FESEM observations

Selected samples containing dolomite were dispersed by ultrasonic treatment in absolute ethanol for five to ten minutes. One or two droplets of the suspension were then deposited directly on an aluminum support for SEM observations, and coated with platinum. The morphology of crystal faces was observed using a Zeiss Ultra 55 field emission gun scanning electron microscope (FESEM) with a maximum spatial resolution of approximately 1 nm at 15 kV.

2.2.2. FTIR measurements

The powdered dolomitic samples were also characterized using infrared spectrometry, with a BRUKER HYPERION 3000 infrared microscope. The infrared beam was focused through a 15× objective and the typical size of the spot on the sample was around $50 \times 50 \mu\text{m}^2$. The spectral resolution was 4 cm^{-1} and the spectra were recorded in transmission option between 4000 cm^{-1} and 500 cm^{-1} . For these measurements, some fine aggregates of dolomitic samples were manually compressed between two KBr windows in order to deposit a thin film of sample on a KBr window.

2.3. Characterization of the interacting solutions

In three dolomite precipitation experiments (runs Dol6, Dol7 and Dol8), about 10 ml of the dispersion were withdrawn from the reactor as a function of time (typically after 1, 3, 5, 8, 24 and 48 h of reaction). The pH was measured directly in the suspension at room temperature using a simple MA235 pH/ion analyzer. About 1 ml of each suspension was then filtered through a $0.2 \mu\text{m}$ Teflon filter. The resulting filtered solutions were acidified with one drop of concentrated HNO_3 solution (3 N) and diluted from 50 to 500 times for measurement of [Ca], [Mg] and [Na] by inductively coupled plasma optical emission spectrometry (ICP-OES). Note that the quenching step of withdrawn suspensions avoids any significant disturbance of the solid reaction products. Conversely, the chemistry of recovered solutions (pH, ion composition and probably ion speciation) can be significantly modified by cooling and/or depressuring events as clearly demonstrated by modelling of calcite precipitation under hydrothermal conditions (Fritz et al., 2013). For this reason, the dolomite formation rate and reaction mechanisms were mainly deduced from solid mineral characterization in the present study.

3. Results and discussion

3.1. Dolomite precipitation: physicochemical steps and reaction mechanism

The precipitation of magnesite and dolomite at ambient temperature is virtually impossible due to strong solvation shells of magnesium ions in aqueous media and probably also due to the existence of a more intrinsic crystallization barrier that prevents the formation of long-range ordered structures at ambient

conditions (Xu et al., 2013). Conversely, dolomite can be easily precipitated at high temperature ($>100 \text{ }^\circ\text{C}$), but its precipitation requires several days or weeks depending on experimental conditions (Grover and Kubanek, 1983; Dockal, 1988; Kaczmarek and Sibley, 2011; Etschmann et al., 2014; Jonas et al., 2015). A simple and novel precipitation route for the formation of rhombohedral single crystals ($<2 \mu\text{m}$) of dolomite is described here. The precipitation process to obtain high-purity dolomite and/or dolomitic material at a temperature ranging from 200 to $300 \text{ }^\circ\text{C}$ requires only 48 h and can be explained by two main sequential steps (see Fig. 1):

- (1) Mg-calcite precipitation at ambient temperature ($\sim 20 \text{ }^\circ\text{C}$) by aqueous carbonation of portlandite ($\text{Ca}(\text{OH})_2$) with CO_2 in a highly alkaline medium (1 M of NaOH and 1 M of MgCl_2). This physicochemical step leads to the precipitation of oriented nanoparticles of low- and high-Mg calcite (79 wt%) coexisting with aragonite (18 wt%) and brucite (3 wt%) after 24 h of solid-fluid interaction as attested by XRD and FESEM observations on the solid (see Fig. 1a).

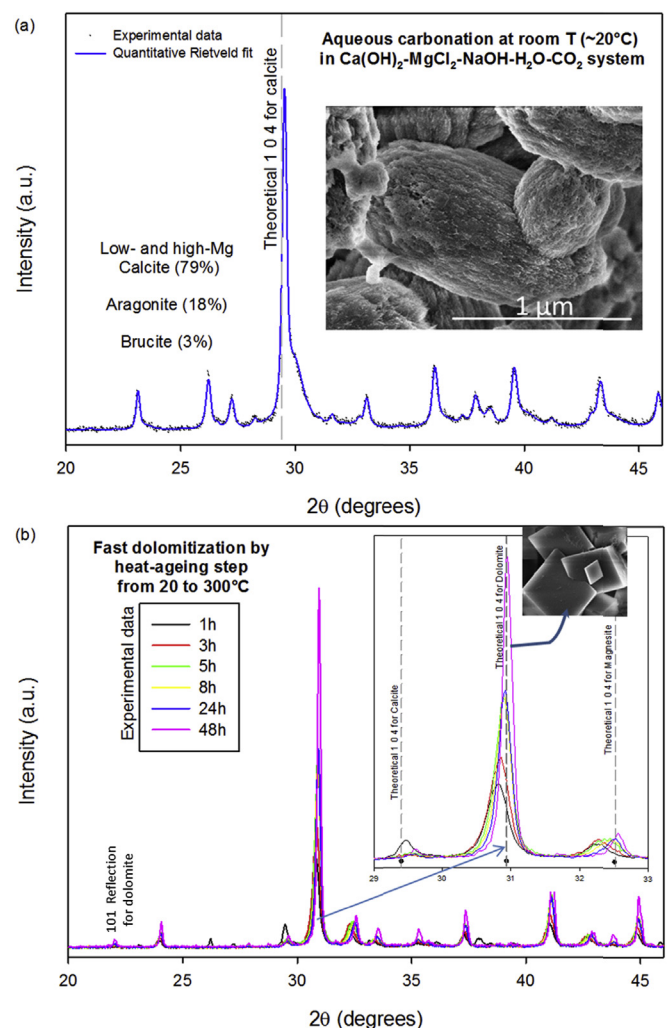


Fig. 1. (a) Experimental XRD pattern and its respective Rietveld fit for solid product obtained at ambient temperature ($\approx 20 \text{ }^\circ\text{C}$) from the $\text{Ca}(\text{OH})_2\text{-MgCl}_2\text{-NaOH-H}_2\text{O-CO}_2$ system, including a FESEM image of magnesium calcite (inset). (b) Experimental XRD patterns for collected time samples after heat-aging step from 20 to $300 \text{ }^\circ\text{C}$ in the dolomitization experiment (run: dol6). FESEM image showing ordered dolomite at the end of the experiment (inset).

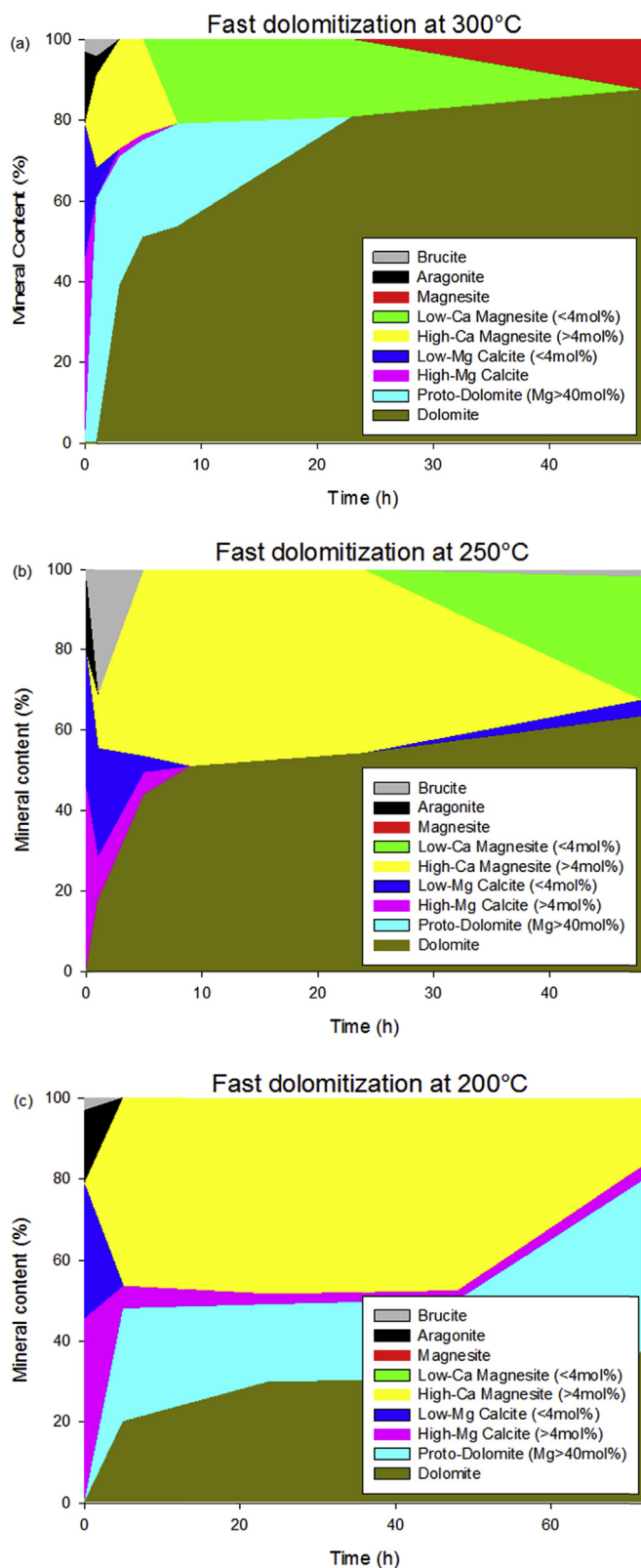


Fig. 2. Time-dependent mineral composition deduced from Rietveld refinement of experimental XRD patterns for dolomitization experiments at 300 °C (a), 250 °C (b) and 200 °C (c).

Assuming that CO_2 absorption in the highly alkaline solution of NaOH is faster and greater than in high-purity water via the following exothermic reaction:

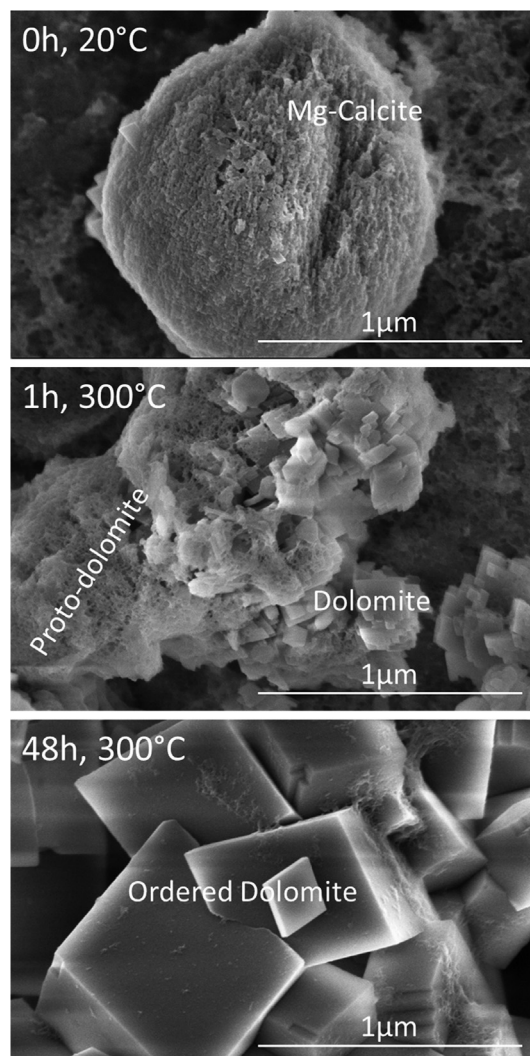
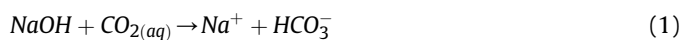
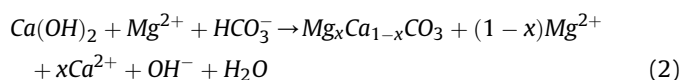


Fig. 3. FESEM images showing Mg-calcite synthesized at ambient temperature, i.e. prior to the heat-ageing step (top), Proto-dolomite and first dolomite particles precipitated after 1 h of reaction, including heating period from 20 to 300 °C (middle), Ordered dolomite obtained at 300 °C for 48 h of reaction (bottom).



the carbonation of portlandite leading to the precipitation of magnesium calcite can be written as follows:



These two coupled reactions take place at ambient temperature (~ 20 °C) for the first 24 h. For simplicity, the formation of minor mineral phases such as aragonite and brucite was excluded from the reaction (2). As shown by experimental measurements, these two reactions are exothermic, with the suspension temperature reaching a maximum value of 29 ± 1 °C after about 1 h of reaction. The maximum value of temperature remains constant for about 2 h and then decreases slowly to ambient temperature (~ 20 °C).

(2) A heat-ageing step from 20 to 200, 250 or 300 °C promotes the dolomitization process, i.e. the transformation of magnesium calcite-rich suspensions to dolomite and/or

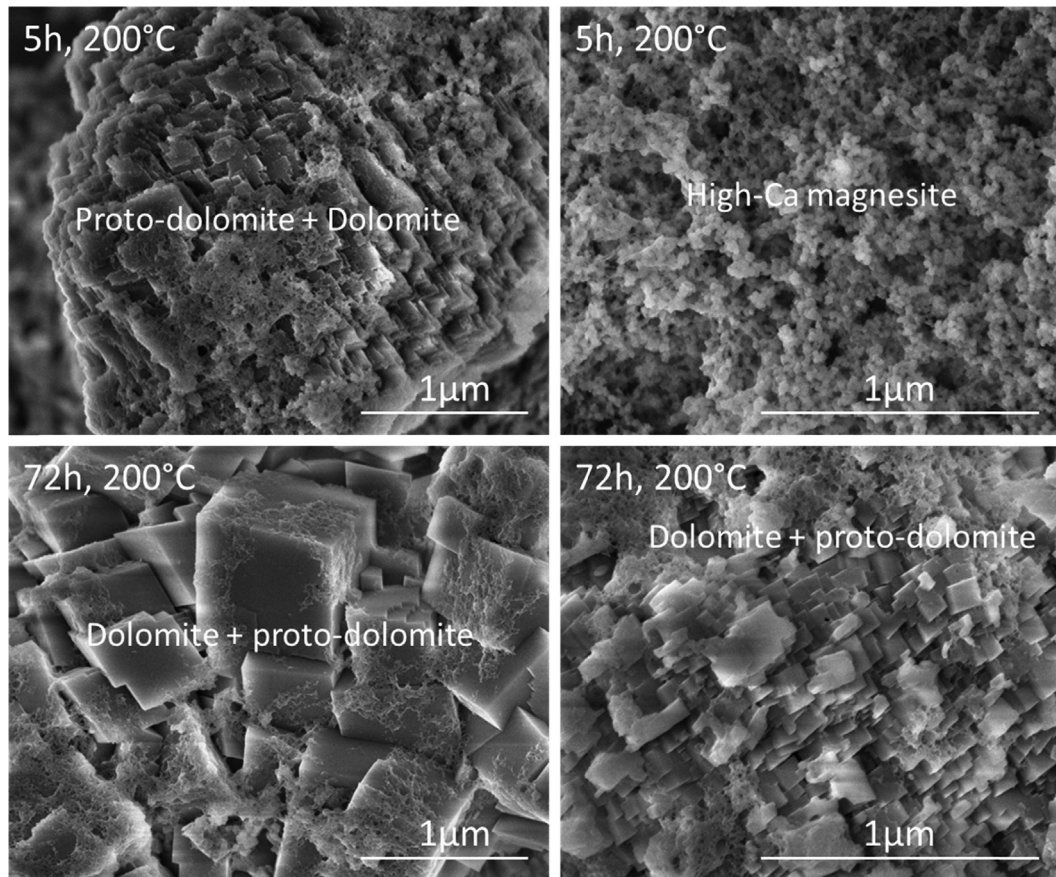
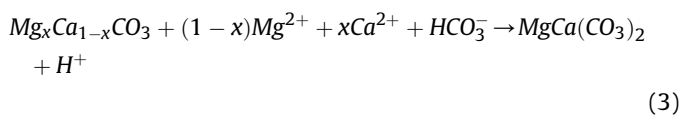


Fig. 4. FESEM images showing proto-dolomite and dolomite (top-left picture) and high-Ca magnesite (Ca content > 4 mol%) (top-right picture) precipitated and/or coexisting at 200 °C after 5 h of reaction, Proto-dolomite and dolomite particles obtained at 200 °C for 72 h of reaction (bottom pictures).

dolomitic material (see for example Fig. 1b: dolomitization process at 300 °C “run Dol6”). The dolomite formation can be expressed as follows:



Note that the proton produced in an ideal reaction (3) is neutralized by the OH^- produced in reaction (2). Moreover, the reaction (3) excludes coexisting mineral phases during dolomitization. Rietveld refinement of XRD patterns for collected time samples has revealed complex kinetic behavior. Dolomite was determined starting from 1 h of reaction (see Fig. 2: runs Dol6 to Dol8), but this co-exists with other carbonate transient mineral phases such as low-Mg calcite (Mg < 4 mol%), high-Mg calcite (Mg > 4 mol%), proto-dolomite or disordered dolomite (Mg > 40 mol%), high-Ca magnesite (Ca > 4 mol%), low-Ca magnesite (Ca < 4 mol%) and magnesite at the investigated condition as displayed in Fig. 2. In general, both the dolomite formation rate and the time-dependent mineral composition depend strongly on reaction temperature (see Fig. 2). For example, high-purity dolomitic material (87 wt% of dolomite mixed with 13 wt% of magnesite) was obtained at 300 °C after 48 h of reaction (Fig. 2a: run Dol6). Conversely, a lower proportion of dolomite (37 wt%) (mixed with proto-dolomite (43 wt%), Ca-magnesite (16 wt%) and high-Mg calcite (4 wt%)) was obtained at 200 °C after 72 h of reaction (Fig. 2c: run Dol7). More specific details on the time-dependent

mineral composition are given in Fig. 2 and Table 1 (runs: Dol6 to Dol8). On the basis of these results, the authors suggest that the formation of dolomite is controlled by dissolution-precipitation reactions, not necessarily coupled in time and space (at grain scale) as deduced from FESEM images (Figs. 3 and 4). In fact, the initial Mg-calcite precipitating at ambient temperature was quickly dissolved at higher temperature (200–300 °C) to form dolomite and other Mg-Ca anhydrous carbonates (including proto-dolomite) (Figs. 3 and 4). These transient mineral phases dissolve in turn to form new dolomite particles or nourish the existent dolomite particles by a crystal growth process. They can also co-exist with dolomite until the end of the experiment as displayed in Fig. 2. Additionally, the magnesium and calcium concentrations in the interacting solutions displayed in Fig. 5a for runs Dol6, Dol7 and Dol8 also support the theory that dissolution-precipitation reactions control the fast dolomite formation because a significant variation in these concentrations was measured in the first hours of reaction. It should also be noted that high calcium and magnesium concentrations were measured at the end of the experiments. For example, calcium concentration is about five times higher than magnesium concentration, thus explaining why dolomite co-exists with magnesite in the experiments where stoichiometric dolomitic composition compounds were exclusively used. These high-concentrations (including Na) are in agreement with pH behavior (near to neutral value) that is mainly controlled by carbonate speciation where HCO_3^- is the dominant species (Fig. 5b).

Dolomite formation rate was determined by plotting the dolomite content (in wt%) against time (h). The resulting curves for the experiments Dol6, Dol7 and Dol8 were fitted using a simple

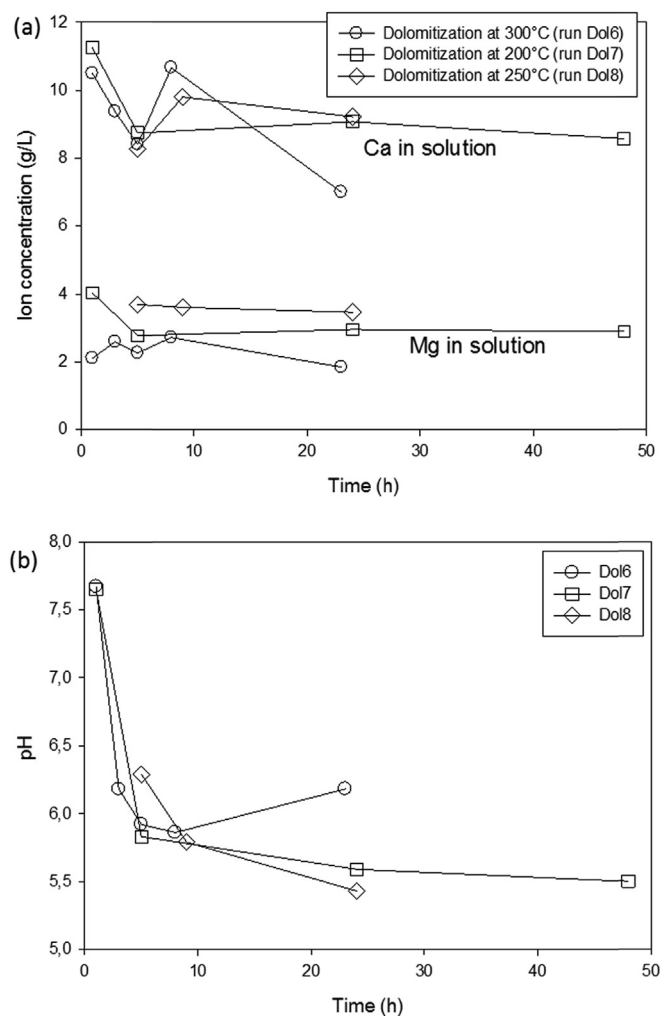


Fig. 5. Ex-situ solution chemistry during dolomite formation at 200, 250 and 300 °C. Calcium and magnesium concentrations (a) and pH (b) as a function of time.

pseudo-second-order kinetic model in order to estimate the initial reaction rate of dolomitization (Fig. 6). Graphically, this initial rate is defined as the slope of the tangent line when the time tends toward zero on the “dolomite content versus time” curve (Montes-Hernandez et al., 2009). The results summarized in Table 2 reveal that the maximum dolomite content is positively correlated with temperature (see Fig. 6 and Table 2). Conversely, the initial rate of dolomitization is not necessary proportional to reaction temperature, probably due to the precipitation-dissolution of transient mineral phases (see Fig. 2 and Table 1). For this case, a similar order of magnitude was calculated for the three investigated temperatures. However, it was confirmed that the high-carbonate alkalinity at high temperature (>200 °C) significantly reduces the energetic barriers to form dolomite in a given system, as explained below.

3.2. Role of temperature

Reaction temperature has a significant influence on the dolomitization kinetics, reaction extent and mineral composition (see Tables 1 and 2). Moreover, the sequential heat-ageing steps performed in run Dol9 revealed that only a small proportion (6 wt%) of proto-dolomite was formed at 90 °C after 4 days of reaction and that magnesium calcite (41 wt%), brucite (37 wt%) and aragonite (10 wt%) are the dominant mineral phases. The second heat-ageing

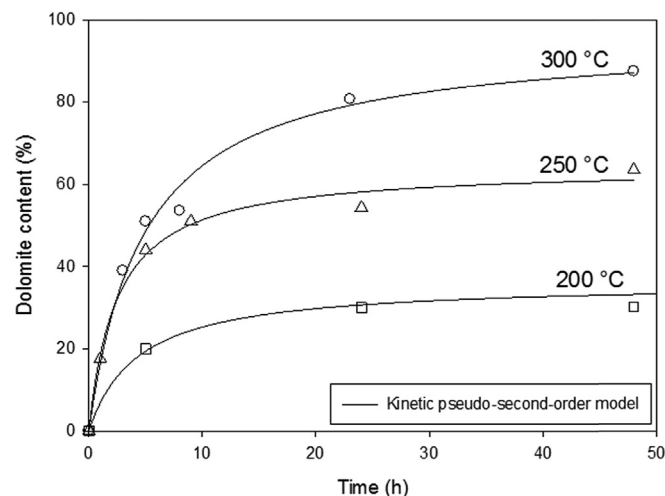


Fig. 6. Kinetic behavior and temperature influence (experimental kinetic data and fitting curves) for ordered dolomite formation from the $\text{Ca}(\text{OH})_2\text{-MgCl}_2\text{-NaOH-H}_2\text{O-CO}_2$ system promoted by a heat-ageing step from 20 to 200, 250 and 300 °C. All fitting parameters are summarized in Table 2.

Table 2

Summary of kinetic parameters for dolomite formation from the $\text{Ca}(\text{OH})_2\text{-MgCl}_2\text{-NaOH-H}_2\text{O-CO}_2$ system promoted by a heat-ageing step from 20 to 200, 250 and 300 °C.

| Temperature (°C) | $\xi_{\text{extent, max}}$ (%) | $t_{1/2}$ h | v_0 1/s | E_a kJ/mol |
|--|--------------------------------|-------------|------------------------|--------------|
| $\text{Mg}_x\text{Ca}_{1-x}\text{CO}_3 + (1-x)\text{Mg}^{2+} + x\text{Ca}^{2+} + \text{HCO}_3^- \rightarrow \text{MgCa}(\text{CO}_3)_2 + \text{H}^+$ | | | | |
| 200 | 36.2 | 4.3 | 2.328×10^{-5} | 5* |
| 250 | 64.2 | 2.5 | 7.146×10^{-5} | |
| 300 | 96 | 4.8 | 5.475×10^{-5} | |

$\xi_{\text{extent, max}}$ is the maximum value of dolomite content at apparent equilibrium and $t_{1/2}$ is the half-content time determined by using a pseudo-second-order kinetic model. v_0 is the initial reaction rate ($v_0 = \xi_{\text{extent, max}}/t_{1/2} \times 100$). E_a : activation energy determined by Arrhenius equation (conventional linear form). *: to be treated with precaution because poor linear correlation ($R \approx 0.8$) exists for $\ln(v_0)$ vs. $1/\text{Temperature}$.

step from 90 to 200 °C promotes dissolution-precipitation reactions, leading to an increase in proto-dolomite formation from 6 to 22 wt% after 24 h of reaction, coexisting mainly with high-Ca magnesite (34 wt%), high-Mg calcite (33 wt%) and aragonite (8 wt%). The final heat-ageing step from 200 to 300 °C obviously leads to the formation of dolomite (51 wt%) after 30 h of reaction which coexists mainly with proto-dolomite (18 wt%), brucite (20 wt%) and magnesium calcite (11 wt%). This final mineral composition at 300 °C is clearly different from the mineral composition obtained at the same temperature with only a single heat-ageing step (Dol6) where the final product is mainly composed of dolomite and magnesite after 24 h. This means that episodic heating-steps can have a significant impact on the reaction pathway and dolomitization extent in hydrothermal systems. For example, Fig. 7 summarizes the dolomitization extent (including proto-dolomite) as a function of temperature for runs Dol6 to Dol9 in which the single heat-ageing step has systematically promoted higher dolomitization with respect to sequential heat-ageing steps in the same experiment (see Fig. 7).

3.3. Role of NaOH and magnesium source

In general, the presence of NaOH promotes the carbonation process and substantially increases the carbonate alkalinity via reaction (1) in our experiments. This carbonate alkalinity reduces

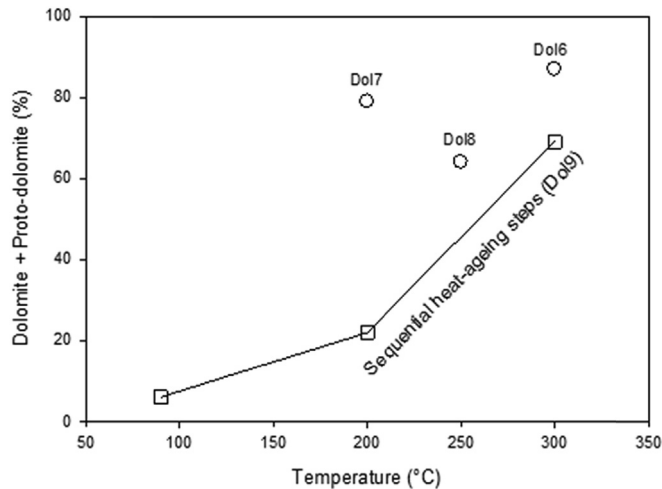


Fig. 7. Dolomite content (including proto-dolomite) from Table 1 as a function of temperature for a single (independent runs: Dol6-to-Dol8) and sequential heat-ageing steps (run Dol9: from 20 to 90 °C, from 90 to 200 °C and from 200 to 300 °C).

the hydration potential of magnesium ions thereby promoting the incorporation of magnesium in calcite at ambient temperature and leading to the precipitation of oriented nanoparticles of magnesium calcite rather than aragonite (see Figs. 1a and 3(top)). This initial precursor formed at ambient temperature is more easily transformed into dolomite by a heat-ageing step from 20 to 300 °C (Dol6-48 h) compared with a similar experiment carried out in absence of NaOH (Dol10). In both cases, ordered dolomite was precipitated (see Fig. 8), but the dolomitization extent is clearly lower in absence of NaOH as reported in Table 1 for runs Dol6 and Dol10. In fact, in absence of NaOH, significant proportion of magnesite co-exists with ordered dolomite at the end of experiments as revealed by XRD (Table 1) and FTIR spectroscopy (Fig. 8: runs Dol6-48 h and Dol10). On the other hand, synthetic $Mg(OH)_2$ (brucite) was also tested as a magnesium source (runs Dol11 and Dol12). Despite brucite is less soluble than $MgCl_2$ and can remain stable at high temperature, high dolomitization extent (75% of dolomite + 16% of proto-dolomite) was determined from XRD pattern after 72 h of reaction for $Ca(OH)_2$ - $Mg(OH)_2$ -NaOH- H_2O - CO_2 system. Conversely, in absence of NaOH, i.e. for $Ca(OH)_2$ - $Mg(OH)_2$ - H_2O - CO_2 system, the dolomitization process was completely inhibited for the same reaction temperature and duration. Herein, magnesite and magnesium calcite were mainly precipitated (see Table 1 and Fig. 7: runs Dol11 and Dol12). This expected result justifies clearly that carbonate alkalinity induces also the dolomite formation at high temperature, as previously demonstrated for dolomite formation via simultaneous dissolution of calcite and magnesite (Montes-Hernandez et al., 2014).

3.4. Geological implications

The present study shows that a heat-ageing step promotes the fast formation of dolomite from magnesium calcite-rich system under high-carbonate alkalinity. On the basis of these experiments an alternative mechanism can be proposed for the formation of massive dolomite bodies in sedimentary environments (ex. deep sea organic-rich carbonate-sediments) if such sediments are subjected to significant temperature variations during burial conditions. This leads to the formation of so-called hydrothermal dolomite that has been frequently observed in carbonate platforms (Davies and Smith). The Latemar platform is a clear example where hot fluids were circulated through carbonates leading to massive

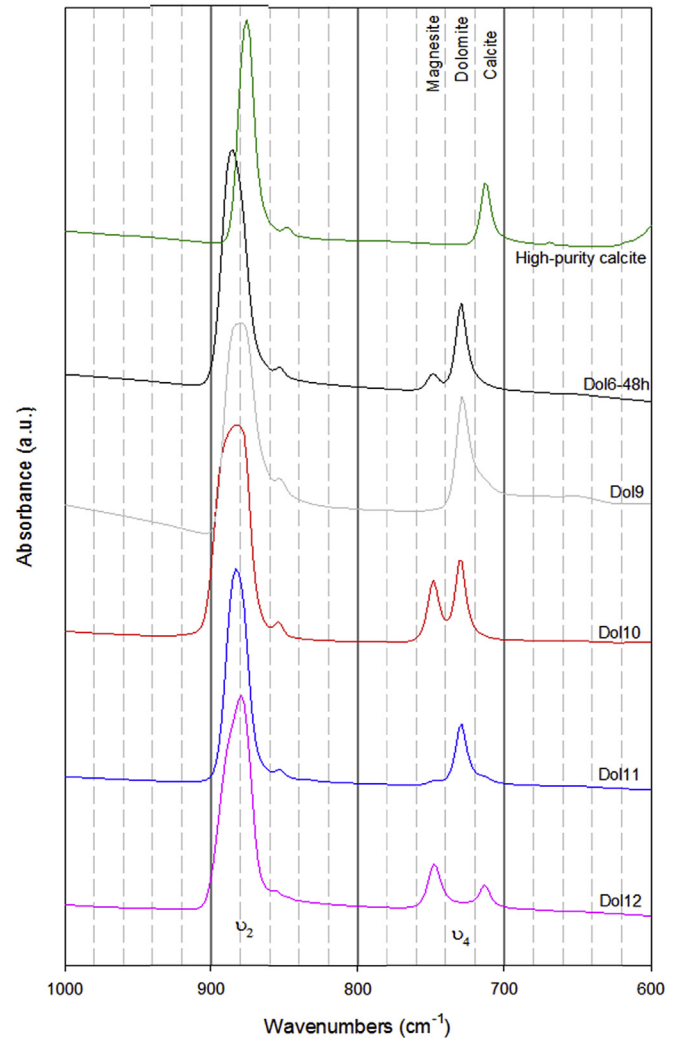


Fig. 8. Fourier transform infrared spectroscopy measurements (in transmission mode) from 1000 to 600 cm^{-1} indicating, in particular, ν_2 and ν_4 vibrational modes for anhydrous Ca-Mg carbonates. High-purity calcite and high-purity dolomite obtained at 300 °C for 48 h (this study: dol6-48 h and dol9) were used as references. Dol10, Dol11 and Dol12 concern three independent experiments also performed at 300 °C for 48 h, but with the following simple variations: Dol10 (in absence of NaOH), Dol11 ($MgCl_2$ replaced by $Mg(OH)_2$), Dol12 (in absence of NaOH and $MgCl_2$ replaced by $Mg(OH)_2$).

dolomitization in relation to fracture-controlled igneous intrusions. Parallel mafic dikes crosscut the Latemar platform forming borders to several of its large dolomite bodies (50 m wide, 100 m high). In this case, the dolomitization is the result of limestone interactions with hydrothermal fluids delivered along these dikes (Jacquemy et al., 2014). This kind of hydrothermal system could also explain the transfer of certain elements of economic interest such as lead, zinc and some rare earth elements (Warren, 2000; Davies and Smith, 2006). Based on this experimental study, it is suggested that the dolomitization process in hydrothermal fields could be a fast reaction if all thermodynamic and physicochemical conditions are combined (T, alkalinity, Mg availability, pre-existent precursors "e.g. Mg-calcite" etc.). Moreover, the mineral replacement of limestone by dolomite is not necessarily an isovolumic process, i.e. the dissolution of primary minerals is not necessarily coupled in time and space with the precipitation of secondary minerals, as frequently assumed for dolomite formation requiring long durations (Dockal, 1988; Malone et al., 1996; Warren, 2000). It may also be concluded that dolomite could easily be formed in the

laboratory at high-temperature (>100 °C), but its precipitation at low temperature (<90 °C) remains a challenge for experimental geochemists and mineralogists. Finally, based on the present experimental study, it can be inferred that many hydrothermal dolomites observed in nature (e.g. saddle dolomite) are systematically ordered, i.e. they are composed of regular alternating monolayers of calcium and magnesium perpendicular to the c-axis (Lippmann, 1973). This simple criterion could be used qualitatively to identify hydrothermal (ordered) dolomites. However, this criterion cannot replace measurements such as stable oxygen (¹⁸O) and carbon (¹³C) isotopes and fluid inclusion re-homogenization temperature and salinity that can quantitatively discriminate between hydrothermal and low-temperature dolomites.

4. Conclusion

In the present study, various experimental simulations were performed to assess how a heat-ageing step promotes the rapid formation of dolomite under high-carbonate alkaline conditions via dissolution-precipitation reactions. The alkaline conditions reduce the hydration of magnesium, enhancing its incorporation into calcite or the direct formation of dolomite. Thanks to the heating step, dolomitization can be achieved within a couple of days. These experiments provide another alternative physicochemical explanation for dolomitization in ancient carbonate platforms where hydrothermal dolomites have been observed, or in active volcanic and hydrothermal fields where carbonates can dissolve or precipitate.

Acknowledgements

The authors are grateful to the French National Center for Scientific Research (CNRS), the Universite Grenoble Alpes, the Labex OSUG@2020 (Investissement d'avenir-ANR10-LABX56), and the ANR French research agency (ANR CORO (ANR-11-BS56-0004) and ANR SPRING (ANR-10-JCJC-0505) projects) for providing funding support.

References

- Arvidson, R.S., Mackenzie, F.T., 1997. Tentative kinetics model for dolomite precipitation rate and its application to dolomite distribution. *Aquat. Geochem.* 2, 273–298.
- Arvidson, R.S., Mackenzie, F.T., 1999. The dolomite problem: control of precipitation kinetics by temperature and saturation state. *Am. J. Sci.* 299, 257–288.
- Blendinger, W., 2004. Sea level changes versus hydrothermal diagenesis: origin of Triassic carbonate platform cycles in the dolomites, Italy. *Sediment. Geol.* 169, 21–28.
- Compton, J.S., 1988. Degree of supersaturation and precipitation of organogenic dolomite. *Geology* 16, 318–321.
- Davies, G.R., Smith Jr., L.B., 2006. Structurally controlled hydrothermal dolomite reservoir facies: an overview. *AAPG Bull.* 90, 1641–1690.
- Deelman, J.C., 2001. Breaking Ostwald's rule. *Chem. Der Erde-Geochemistry* 61, 224–235.
- Deelman, J.C., 2011. Low-temperature Formation of Dolomite and Magnesite, pp. 211–273. ISBN 9-809803-1-5. <http://www.jcdeelman.demon.nl/dolomite/bookprospectus.html>.
- Deng, S., Dong, H., Lv, G., Jiang, H., Yu, B., Bishop, M.E., 2010. Microbial dolomite precipitation using sulfate reducing and halophilic bacteria: results from Qinghai lake, Tibetan Plateau, NW China. *Chem. Geol.* 278, 151–159.
- Dockal, J., 1988. Thermodynamic and kinetics description of dolomitization of calcite and calcitization of dolomite (dedolomitization). *Carbonates Evaporites* 3, 125–141.
- Etschmann, B., Brugger, J., Pearce, M.A., Ta, C., Brautigan, D., Jung, M., Pring, A., 2014. Grain boundaries as microreactors during reactive fluid flow: experimental dolomitization of a calcite marble. *Contrib. Mineral. Petrol.* 168, 1045.
- Fritz, B., Clement, A., Montes-Hernandez, G., Noguera, C., 2013. Calcite formation by hydrothermal carbonation of portlandite: complementary insights from experiment and simulation. *CrystEngComm* 15, 3392–3401.
- Grover, J., Kubanek, F., 1983. The formation of ordered dolomite from high-magnesium calcite at 250 to 350 °C and 1500 bars: epitaxial growth with optimal phase orientation and implications for carbonate diagenesis. *Am. J. Sci.* 283, 514–539.
- Jacquemyn, C., El Desouky, H., Hunt, D., Casini, G., Swennen, R., 2014. Dolomitization of the Latemar platform: fluid flow and dolomite evolution. *Mar. Petrol. Geol.* 55, 43–67.
- Jonas, J., Müller, T., Dohmen, R., Baumgartner, L., Putlitz, B., 2015. Transport-controlled hydrothermal replacement of calcite by Mg-carbonates. *Geology* 43, 779–782.
- Kaczmarek, S., Sibley, D.F., 2011. On the evolution of dolomite stoichiometry and cation order during high-temperature synthesis experiments: an alternative model for the geochemical evolution of natural dolomites. *Sediment. Geol.* 240, 30–40.
- Kenward, P.A., Goldstein, R.H., Gonzalez, L.A., Roberts, J.A., 2009. Precipitation of low-temperature dolomite from anaerobic microbial consortium: the role of methanogenic Archea. *Geobiology* 7, 556–565.
- Krause, S., Liebetrau, V., Gorb, S., Sanchez-Roman, M., Mackenzie, J.A., Treude, T., 2012. Microbial nucleation of Mg-rich dolomite in exopolymeric substances under anoxic modern seawater salinity: new insight into an old enigma. *Geology* 40, 587–590.
- Lippmann, F., 1973. *Sedimentary Carbonate Minerals*. Springer-Verlag, 228pp.
- Machel, H.G., 2001. Bacterial and thermochemical sulfate reduction in diagenetic setting-old and new insights. *Sediment. Geol.* 140, 143–175.
- Malone, M.J., Baker, P.A., Burns, S.J., 1996. Recrystallization of dolomite: an experimental study from 50 to 200 °C. *Geochim. Cosmochim. Acta* 60, 2189–2207.
- McKenzie, J.A., 1991. The dolomite problem: an outstanding controversy. In: Muller, D.W., McKenzie, J.A., Weissert, H. (Eds.), *Controversies in Modern Geology: Evolution of Geological Theories in Sedimentology*. Academic Press, London, pp. 37–54.
- McKenzie, J.A., Vasconcelos, C., 2009. Dolomite mountains and the origin of the dolomite rock of which they mainly consist: historical developments and new perspectives. *Sedimentology* 56, 205–219.
- Medlin, W.L., 1959. The precipitation of synthetic dolomite. *Am. Min.* 44, 979–986.
- Montes-Hernandez, G., Findling, N., Renard, F., Auzende, A.-L., 2014. Precipitation of ordered dolomite via simultaneous dissolution of calcite and magnesite: new experimental insights into an old precipitation enigma. *Cryst. Growth Des.* 14, 671–677.
- Montes-Hernandez, G., Fernandez-Martinez, A., Renard, F., 2009. Novel Method to estimate the linear growth rate of submicrometric calcite produced in a triphasic gas-liquid-solid system. *Cryst. Growth Des.* 9, 4567–4573.
- Nash, M.C., Troitzsch, U., Opdyke, B.N., Trafford, J.M., Russell, B.D., Kline, D.L., 2011. First discovery of dolomite and magnesite in living coralline algae and its geobiological implications. *Biogeosciences* 8, 3331–3340.
- Pimentel, C., Pina, C.M., 2014. The formation of the dolomite-analogue norsethite: reaction pathway and cation ordering. *Geochim. Cosmochim. Acta* 142, 217–223.
- Sanchez-Roman, M., McKenzie, J.A., Wagoner, A.-de-L.R., Rivasdoneyra, M.A., Vasconcelos, C., 2009. Presence of sulfate does not inhibit low-temperature dolomite precipitation. *Earth Planet. Sci. Lett.* 285, 131–139.
- Taut, T., Kleeberg, R., Bergmann, J., 1998. The new Seifert Rietveld program BGMN and its application to quantitative phase analysis. *Mater. Sci. Bull. Czech Slovak Crystallogr. Assoc.* 5, 55–64.
- Warren, J., 2000. Dolomite: occurrence, evolution and economically important associations. *Earth-Sci. Rev.* 52, 1–81.
- Warthmann, R., Van Lith, Y., Vasconcelos, C., McKenzie, J.A., Karpoff, A.M., 2000. Bacterially induced dolomite precipitation in anoxic culture experiments. *Geology* 28, 1091–1094.
- Xu, J., Yan, C., Zhang, F., Konishi, H., Xu, H., Teng, H., 2013. Testing the cation-hydration effect on the crystallization of Ca-Mg-CO₃ systems. *PNAS*. <http://dx.doi.org/10.1073/pnas.1307612110>.